CHARGED PHOTOPARTICLES FROM ARGON

by

MICHAEL ANDREW REIMANN

B.A.Sc., University of British Columbia, 1959

A thesis submitted in partial fulfilment of the requirements for the degree of

MASTER OF APPLIED SCIENCE

in

PHYSICS

We accept this thesis as conforming to the required standard

THE UNIVERSITY OF BRITISH COLUMBIA

April, 1964

In presenting this thesis in partial fulfilment of the requirements for an advanced degree at the University of British Columbia, I agree that the Library shall make it freely available for reference and study. I further agree that permission for extensive copying of this thesis for scholarly purposes may be granted by the Head of my Department or by his representatives. It is understood that copying or publication of this thesis for financial gain shall not be allowed without my written permission.

Department of PHYSICS

The University of British Columbia,
Vancouver 8, Canada

Date 6 May 1964

ABSTRACT

The energy distribution of charged photoparticles from the interaction of the A^{40} nucleus with 17.64 Mev and 14.7 Mev gamma rays from the reaction $Li^{7}(p,\gamma)Be^{8}$ has been obtained using a gridded ionization chamber. A total cross section of 5.8 mb. was found for the combined production of photoprotons and photoalphas. Peaks in the energy spectrum corresponding to photoproton events leading to the ground and first excited states of the residual nucleus Cl^{39} were identified but some features of the energy distribution remain unexplained.

ACKNOWLEDGEMENTS

The author is pleased to express his sincere gratitude to Dr. J.B. Warren for his kind supervision of this research project. The guidance of Dr. B.L. White and Dr. G. Jones in various aspects of the work is greatly appreciated.

In particular, the author wishes to thank Mr. J.R. MacDonald for his countless helpful suggestions, his willing assistance in operating the Van de Graaff accelerator, his lasting interest in the project, and for many stimulating discussions late at night.....

The author is deeply indebted to the National Research Council of Canada for the two scholarships held during the course of this work, and for their continued financial support.

TABLE OF CONTENTS

Table of Contents (cont.-)

LIST OF FIGURES

LIST OF TABLES

PROLOGUE

It happened on a midnight clear
The Machine - it worked! Results were near ...
Coincidence beyond belief
Caused happy smiles, not breakdown grief.
Diffusion pumps sucked side by side
While amplifiers amplified.
Then, as proton beam came down
The Magnet deftly bent it round,
The Sniffers let the beam go by
And gamma rays began to fly.
Scintillators scintillated,
The Integrator integrated,
The Sorter kicked, the Scaler scaled -
(Not even a transistor failed!)
Then, as early morning clock struck three
Results were there for all to see.
To end those weeks of weary toil
Ridding pumps of dirty oil
A change has come we won't resist ....
From technician back to PHYSICIST!

INTRODUCTION

The interaction of electromagnetic radiation with atoms has been of paramount importance in advancing our understanding of atomic structure. It might therefore be expected that the electromagnetic interaction would also provide a powerful tool for study of the structure of the nucleus. The value of the photon as a nuclear probe is enhanced because the electromagnetic force is well understood, unlike the much stronger nuclear force. One method of studying the interaction of photons with nuclear matter is via photodisintegration reactions. These involve the absorbtion of a photon by a nucleus in its ground state, and its subsequent decomposition into two or more particles.

The comprehensive investigation by Hirzel and Wäffler, 1947, of photoprotons from nuclei in the range $Z = 25$ to $Z = 118$ has been followed by a substantial volume of further experimental work (Toms, 1955). However, there remains a remarkable paucity of good experimental data, due to the lack of a sufficiently good source of gamma rays. Available sources are of two types: nuclear reactions induced by particle bombardment, and bremsstrahlung derived from energetic electron beams.

Reaction sources have the advantage of narrow line width, but are generally of low intensity, and often comprise

two or more components of different energy. They have the further disadvantage of being limited to a few discreet energies variable only by choice of reaction, with a maximum of 20.6 Mev from $T(p,\gamma)He^4$. Bremsstrahlung, on the other hand, can be provided with ample intensity and is continuously variable in its maximum energy. It is, however, a "white" radiation source, the shape of whose energy spectrum must be determined in order to interpret the results of photodisintegration experiments for which it is used.

In general, measurement of the energy of radiation useful as a nuclear probe is not nearly as accurate as that which made optical frequency radiation so invaluable for the study of atomic physics. The frequencies of interest in nuclear work are much higher, and the precise techniques of optical spectroscopy must be replaced by less satisfactory indirect methods (Blatt and Weisskopf, 1952).

While the theory of two body photodisintegration has become one of the cornerstones of nuclear physics, the interpretation of the photodisintegration of heavier nuclei is much more complex and relatively uncertain. The gross structure of all photodisintegration cross sections exhibits a "giant resonance" directly attributable to the gamma ray absorbtion cross section of the nucleus. The cross section is peaked between 10 and 25 Mev, and is typically between

3 and 8 Mev wide. It is almost entirely due to electric dipole absorbtion. The theory of this phenomenon is treated in most nuclear physics textbooks, for instance, Blatt and Weisskopf, 1952.

Attempts to interpret such details of the photonuclear break-up as energy and angular distribution of the products as well as the branching ratios involved, have been in terms of two models. These are the usual compound nuclear model of reaction theory and a direct photoeffect model.

In the compound nuclear model the cross section for a given photodisintegration reaction is taken as the product of two independent factors. These are the cross section for formation of the compound nucleus by gamma absorbtion (resulting in the characteristic "giant resonance"), and the probability of its decay by particle emission through the channel of interest. The latter is principally influenced by the barrier penetrability, and thus favours the emission of neutrons over protons. The mechanism of the decay of the compound nucleus by particle emission has been described by Weisskopf, 1937, and Weisskopf and Ewing, 1940, as analogous to the evaporation of molecules from a hot surface. The latter phenomenon is described by a statistical (Maxwell)distribution of the kinetic energy of the evaporated molecules, with the surface temperature as a parameter. In the nuclear case, a particle is "evaporated" from the excited compound nucleus. The energy distribution of the outgoing

particles is largely determined by the energy distribution of the levels in the residual nucleus. On the assumptions that the excitation energy is sufficient to populate levels in the residual nucleus in a region where the level density is great, and that the level density increases rapidly with energy, the energy spectrum of the emitted particles also has the shape of a Maxwell distribution. The analogy to surface evaporation then leads to the definition of a "nuclear temperature" as a parameter of the distribution.

According to the work of Bethe, 1937, the maximum yield of charged particles from the decay of a compound nucleus should occur at an exit channel energy approximately equal to the Coulomb barrier height. This is shown to be true for the predicted energy distribution of photoprotons based on the statistical model, by the calculations of Spicer, 1955.

The statistical model predicts that the majority of particles will be emitted with an exit channel energy well below the maximum allowed by the reaction Q-value. This also favours the emission of neutrons over charged particles because of the dependence of Coulomb barrier penetrability upon channel energy. The model therefore indicates a very small (10^{-2} to 10^{-5}) ratio of photoproton to photoneutron cross sections. In those cases where the particle is emitted with less than maximum energy there is, of course, further de-excitation of the residual nucleus along energetically open channels. These may include emission of another particle, or

gamma decay. Photodisintegrations involving the emission of two particles must therefore be duly considered. One does not expect to be able to apply the statistical model to nuclei so light that the assumption of high level density at the excitation energy of the residual nucleus is unreasonable. It has been used with some success for as low a mass number as 27 by Diven and Almy, 1950.

The accumulated experimental evidence is for a rather larger ratio of photoproton to photoneutron cross section than predicted by the statistical theory. Schiff, 1948, proposes that this might still be explained in terms of that model if a modified energy level density is assumed in the residual nucleus. He gives some justification for this assumption, and shows how this increases the mean exit channel energy of the photoparticles, and consequently changes the photoproton to photoneutron ratio.

The direct photoemission process was postulated by Jensen, 1948, and Courant, 1950, as an alternative explanation for the unexpectedly large photoproton yield. In the direct process a particle is ejected from the target nucleus without the prior formation of a compound nucleus. In such a case all the energy available from the photodisintegration reaction appears as kinetic energy in the exit channel, and the residual nucleus is left in its ground state. The absorbtion of a gamma quantum by a single nucleon in this manner would not always lead to the direct emission of

that nucleon. It might head into the nucleus and lose energy by collision resulting in formation of the compound nucleus as described above. The result of direct effect events, however, is expected to be an energy distribution of photoparticles with the main group at the maximum exit channel energy. This increases the Coulomb barrier penetration probability for charged particles and tends to increase the photoproton to photoneutron ratio. This theory also predicts an anisotropy in the angular distribution of the direct photoparticles, favouring emission at right angles to the incident gamma flux. Courant points out that the direct photoprocess need only have a small cross section relative to that for the formation of the compound nucleus in order to account for the observed photoproton cross section.

Neither theory can entirely account for the experimental results, and so the consideration of both mechanisms in conjunction suggests itself. This possibility was explored by Toms and Stephens, 1953, as an explanation of their results for the photodisintegration of indium, cerium and bismuth. In these heavier nuclei they expected the yield of "evaporated" protons to be greatly reduced due to the increased Coulomb barrier. They calculated the yield of photoprotons and their expected energy distribution using both the statistical and direct photoeffect theories. They matched the two calculated energy distributions to their

experimental curves, combining them in proportions for optimum fit. The observed particle yields from the two processes were found to be in fair agreement with the calculated ones. They were able to interpret these results as definite evidence of an appreciable direct photoproton yield. The observed angular distributions were not as readily resolved, as their anisotropy was not purely that expected from the direct effect protons.

The Photodisintegration of Argon.

The reactions most likely to occur in the photodisintegration of argon are given in Table 1, together with their Q-values as computed from the mass difference tables of Everling et al, 1960, and as tabulated by Bromley and Rutlege, 1958. It is noted that there is some disagreement between these sources, especially for the Q-value of the reaction $A^{40}(\gamma,p)Cl^{39}$. For this reaction the Q-value quoted in the later literature is 12.44 Mev. (See for instance, McPherson et al, 1954.) Pertinent energy level diagrams for the most important reactions are given in Appendix D.

TABLE 1

Q-VALUES FOR THE PHOTODISINTEGRATION OF ARGON

REACTION	Q-VALUES (Mev)		CHANNEL OPEN FOR EXCITATION ENERGY 17.64 MEV MARKED *
	EVERLING ET AL	BROMLEY AND RUTLEGE	
$A^{40}(\gamma,p)Cl^{39}$	- 12.52	- 12.03	*
$A^{40}(\gamma,\alpha)S^{36}$	- 6.81	- 6.76	*
$A^{40}(\gamma,n)A^{39}$	- 9.79	- 9.85	*
$A^{40}(\gamma,d)Cl^{38}$	- 18.37	- 18.30	
$A^{40}(\gamma,t)Cl^{37}$	- 18.26	- 18.15	
$A^{40}(\gamma,He^{3})S^{37}$	- 22.99	- 22.33	
$A^{40}(\gamma,np)Cl^{38}$	- 20.59	- 20.53	
$A^{40}(\gamma,nn)A^{38}$	- 16.45	- 16.49	*
$A^{40}(\gamma,n\alpha)S^{35}$	- 18.35		
$A^{40}(\gamma,\alpha\alpha)Si^{32}$	- 15.69		*
$A^{40}(\gamma,pp)S^{38}$	- 22.82		
$A^{36}(\gamma,p)Cl^{35}$	- 8.51	- 8.65	*
$A^{36}(\gamma,\alpha)S^{32}$	- 6.64	- 6.65	*

The photodisintegration of argon has been studied using a variety of experimental techniques. Following the original work of Wilkinson and Carver, 1951, using gamma rays from the reaction $Li^7(p,\gamma)Be^8$, the majority of experiments were done using bremsstrahlung sources. The first of these is reported by Spicer, 1955.

Wilkinson and Carver obtained an energy distribution of charged photoparticles from photodisintegrations initiated by 14.7 and 17.64 Mev gamma rays. They found no significant contribution which they could attribute to photoalpha particles, and their photoproton excitation function shows a broad peak at 2.5 Mev, an unresolved peak at approximately 4 Mev, and two small peaks at 5.7 and 6.8 Mev. A photostat of their paper appears as Appendix A. The two peaks at 5.7 and 6.8 Mev were identified as full energy peaks corresponding to the first excited and ground states respectively, of the product nucleus Cl^{39}. From varying the flux ratio of 14.7 to 17.6 Mev gammas they concluded that their results were almost entirely due to the 17.6 Mev radiation. They further concluded from the ratio of the 3 photoproton peaks observed in their energy distribution, that the bulk of the disintegration was not due to the direct photoeffect. Their energy distribution was peaked at a lower energy than that expected from the statistical theory.

Spicer's work was done with 22.5 Mev bremsstrahlung. He obtained an energy distribution for photoprotons which is

peaked at 2.6 Mev. Although the majority of absorbed photons were presumed to be of energy close to 20 Mev, his distribution showed negligible yield between proton energies of 7 and 8 Mev where direct photoprotons might be expected. He obtained an excellent fit to his data using the statistical theory with a modified energy level density dependence on energy, and with a Coulomb barrier reduced in height from the classical $Z/A^{1/2}$ by almost 50%. Such a low Coulomb barrier is thought plausible from the work of Scott, 1954. Spicer's angular distribution is strongly anisotropic, peaked at approximately 70° to the incident gamma flux independent of the proton energy.

Later workers have been largely concerned with the determination of the cross sections for photodisintegration reactions and their dependence upon photon energy.

Apart from the theoretical interpretation of the general characteristics of the photodisintegration of argon in terms of the two models, there are several features of the results of Wilkinson and Carver which are not clear, and which have not been resolved by other researchers. Primary among these is the nature of the two peaks in their photoparticle energy spectrum at 5.7 and 6.8 Mev. The identification of these as representing transitions to the ground and first excited states of Cl^{39} is in serious disagreement with the presently accepted Q-value for the reaction as shown in Table 1. Also unexplained among the results of Wilkinson

and Carver is the unresolved group at 4 Mev. In addition, there exists a discrepancy in the cross sections measured by Wilkinson and Carver and by McPherson et al, 1954, of the order of 300%. Spicer's photoproton cross section agrees with that of McPherson et al, and is approximately 15 mb. at 17.6 Mev, while that of Wilkinson and Carver is given as 5.4 mb.

In the present experiment the work of Wilkinson and Carver has been repeated, using a gridded ionization chamber in place of their proportional counter, thus obtaining a much better energy resolution. By this expedient it was hoped to resolve the aforementioned inconsistancies.

CHAPTER I

THE GRIDDED IONIZATION CHAMBER

A. Choice of Detector

Five general methods have been used for the detection of photodisintegration events in argon. These are:

(a) Determination of the residual activity due to the beta-decay of Cl^{39} produced in the reaction $A^{40}(p,\gamma)Cl^{39}$. See for instance McPherson et al, 1954, Brix et al, 1959, and Dosch et al, 1960.

(b) Charged particle track analysis in photographic emulsions. See for instance Spicer, 1955, and Iavor, 1958.

(c) Charged particle track analysis in a Wilson Cloud Chamber, as used by Gudden and Eichler, 1958.

(d) Pulse analysis using a proportional counter, as done by Wilkinson and Carver, 1951.

(e) Pulse analysis using a gridded ionization chamber as done by Komar et al, 1961, for the investigation of the reaction $A^{40}(\gamma,\alpha)S^{36}$.

Method (a) is only useful for cross section measurements, and yields no information about the energy distribution of the

photoprotons. Furthermore, it is only useful in conjunction with a high gamma flux so that the decay of the product Cl^{39} (half life 55 m) taking place during the irradiation is not too large a fraction of the total yield. This technique has therefore only been used with betatron and synchroton bremsstrahlung sources.

The use of photographic emulsions, method (b), has the advantage of yielding information about the angular distribution and the energy of the charged photoparticles as well as indicating the cross section. However, the gas pressure of the argon must be kept low and the volume small, in order to minimize the energy loss of the charged particles by ionization in the gas. This restriction again favours use of high flux gamma sources to yield an adequate number of counts within a reasonable time.

The use of a Wilson Cloud Chamber, (c), once again requires a large gamma flux owing to the brief time for which it is sensitive during its cycle of operation.

The proportional counter, (d) is useful with a low gamma flux, such as that available from particle induced reactions utilizing primary particles from a Van de Graaff generator. It has the advantage of noiseless gas amplification, but this requires a region of high electric field in the neighbourhood of the collector. With the usual cylindrical geometry this, in turn, requires that the collector diameter be small to avoid the problems of having to supply

an extremely high voltage. The field near the counter walls is consequently quite low for a chamber of reasonable diameter, and this has the disadvantage of favouring recombination of ions in the particle tracks with electrons before collection, thus decreasing the energy resolution.

In the case of the gridded ionization chamber (e), which has similar geometry to the proportional counter, a larger diameter collector may be used because there is no high field requirement for gas multiplication. For a given supply voltage this results in a larger field near the chamber walls, which is less favourable for recombination. The grid, which is discussed by Gillespie, 1953, and Monier, 1950, has the effect of making the rise time of the voltage pulses at the collector dependent only on the electron collection time by shielding the collector from the slower positive ions. The rise time is thus equivalent to that of the proportional counter. In addition, the absence of gas gain makes the counter more stable to the presence of impurities in the gas than is the case with proportional counters, particularly at the high pressures needed for adequate stopping power.

The foregoing considerations indicate the suitability of the gridded ionization chamber for the present work. A futher incentive was the successful use of such a chamber for the photodisintegration of neon by Hay and Warren, 1959, and the subsequent availability of their chamber.

B. Details of Chamber Construction

The details of construction are given both by Hay and Warren in their paper (1959), and by Monier, 1960, who used the same chamber for the neutron disintegration of neon. The diagram of the chamber given as Figure 1 is reproduced from the earlier reference. Some of the pertinent details are recalled in Table 2.

TABLE 2

CHAMBER DETAILS

Collector diameter	0.635 cm ($^1/4$ inch)
Grid diameter	1.905 cm ($^3/4$ inch)
Diameter of sensitive volume	15.7 cm
Length of sensitive volume	22.7 cm
Wall area of sensitive volume	1120 cm^2
Sensitive volume	4.40 litres
Wall thickness	0.318 cm
Diameter of grid wires	0.07 cm (30 wires)
Energy of calibrating source	5.15 Mev (Pu^{239})

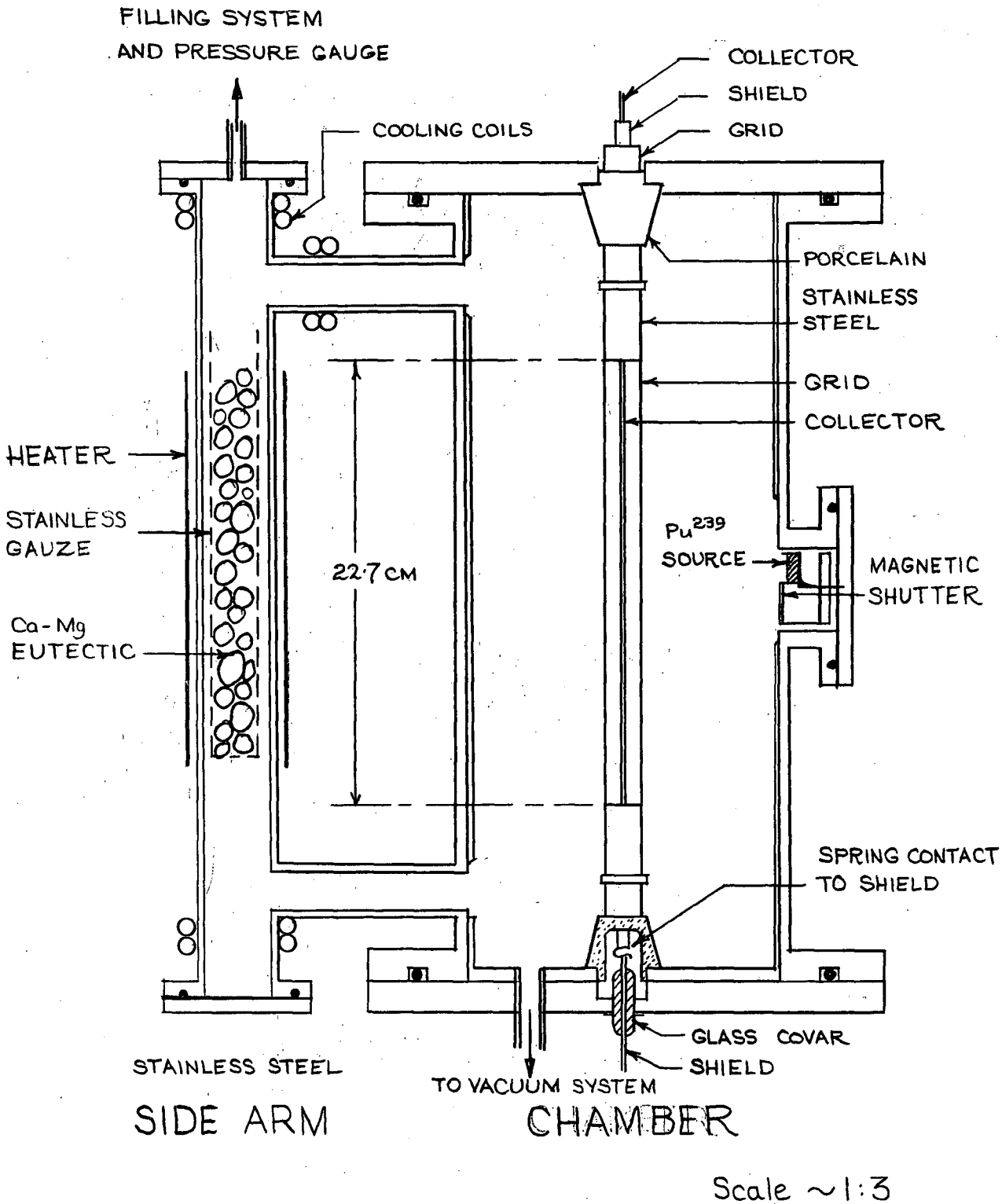

FIGURE 1 The Gridded Ionization Chamber.

See Table 2 for Dimensions.

In place of the calcium turnings used for gas purification by Hay and Warren, 1959, calcium-magnesium alloy was used as described by Colli, 1952. This is more active than pure calcium, and requires less heating. The graphite coating on the inside of the chamber walls used in the previous experiments was not used in this instance. Only the collector and the grid wires were graphite coated. The reason for this is fully discussed in Chapter IV.

C. Method of Operation

(1) Pressure

The optimum operating conditions for the chamber must be determined between two conflicting requirements. On the one hand it is desirable to have good energy resolution. This is favoured by low gas pressure, which reduces collection time and hence the effect of random track orientation, and which reduces the recombination probability. On the other hand, it is essential to keep the track length of the photoparticles as short as possible so that a majority of them lose all their energy in the gas without hitting the walls or moving out of the sensitive volume (wall effect). Reduction of wall effect requires increased pressure. An additional advantage of higher pressure is, of course, an increased count rate for a given gamma flux.

In view of these considerations it was decided to operate the chamber at a pressure of 100 p.s.i. absolute. At this pressure, after purifying briefly, it was found possible to achieve a resolution of 4.0%. The wall effect was still significant (see Appendix B) at this pressure, but the recombination rate was not yet excessive (evidenced by only a slight drop in pulse height from the calibrating source over its low pressure value). The pressure could not conveniently be increased further owing to the strength of the chamber walls. At 100 p.s.i. absolute the range of a 5 Mev proton is approximately 5 cms, and that of a 5 Mev alpha particle 0.63 cm.

(2) Voltage

The collector voltage was established by observing the performance of the chamber as a detector for the alpha particles from the Pu^{239} calibrating source (5.15 Mev) as a function of voltage. As the voltage was increased from a low value, the peak pulse height due to the alphas increased. This was due to the reduction of ion recombination before collection, and was strongly voltage dependent up to a certain maximum voltage associated with complete collection. This was 3 kv. at 100 p.s.i. absolute. Thereafter further increases in voltage produced only slight increases in pulse height as indicated by kicksorter analysis.

This effect was attributed to the increased electron mobility, and was not significant. It was therefore decided to operate at 3 kv, as unnecessarily high voltage only contributes additional noise. For a pressure of 80 p.s.i. absolute a voltage of 2.5 kv. was found sufficient.

The grid voltage was set at one half of the collector voltage. This was in accordance with the findings of Hay and Warren, 1959 for this chamber, and in agreement with the discussion given by Robertson, 1963. Hay and Warren calculated the grid shielding efficiency to be 96% and the electron transparency to be unity under these conditions.

(3) Filling

Before the chamber was filled with argon, it was pumped down to a pressure of $5(10^{-6})$ torr with the calcium-magnesium purifier heated to 500°C to ensure adequate outgassing. The chamber itself was initially outgassed by pumping for several days while being heated with a flexible, insulated heating element. This had to be done, however, before the Mylar lining (see Chapter IV) was inserted, to avoid distortion of this plastic and consequent uncertainty in the sensitive volume.

The purifier was then allowed to cool to 450°C and the argon was admitted directly from the gas bottle. The purifier was kept at 450°C for about one hour and then

turned off. The purpose of the purifier was to remove traces of oxygen and water vapour from the gas as these, even in minute quantities, foster recombination and hence spoil the energy resolution. A liquid nitrogen cold trap in the filling system made no difference to the resolution, even without use of the purifier, and hence its use was discontinued.

The gas used was high grade welding argon quoted at 99.98% argon, of which 99.6% is A^{40} and the remainder A^{36}. The most probable impurities in the cylinder argon besides oxygen and water vapour are nitrogen, hydrogen and carbon dioxide. The eutectic mixture is also effective in removing these, as demonstrated by Colli, 1952.

CHAPTER II

PULSE ANALYSIS

A. General Arrangement

A schematic diagram of the arrangement used for the amplification and analysis of the pulses from the ionization chamber appears as Figure 2. The high voltage supply and the Dynatron amplifying system are discussed under separate headings below. The amplified pulses were analyzed by one half of a Nuclear Data Model ND 103 256 channel kicksorter, this having the facility enabling it to be operated as two independent 128 channel kicksorters.

B. High Voltage Arrangement

High voltage to the collector of the ionization chamber was provided by a Northeast Scientific Corporation High Voltage Power Supply Model ZRE 5001AW1. In view of the very small current required, it was possible to introduce a high impedance, low pass filtering network comprising R_1, R_2, C_1, and L in Figure 3. This was located inside a copper shield directly above the chamber.

Gillespie, 1953, has shown that greater benefit can be obtained from differentiation pulse shaping if it takes

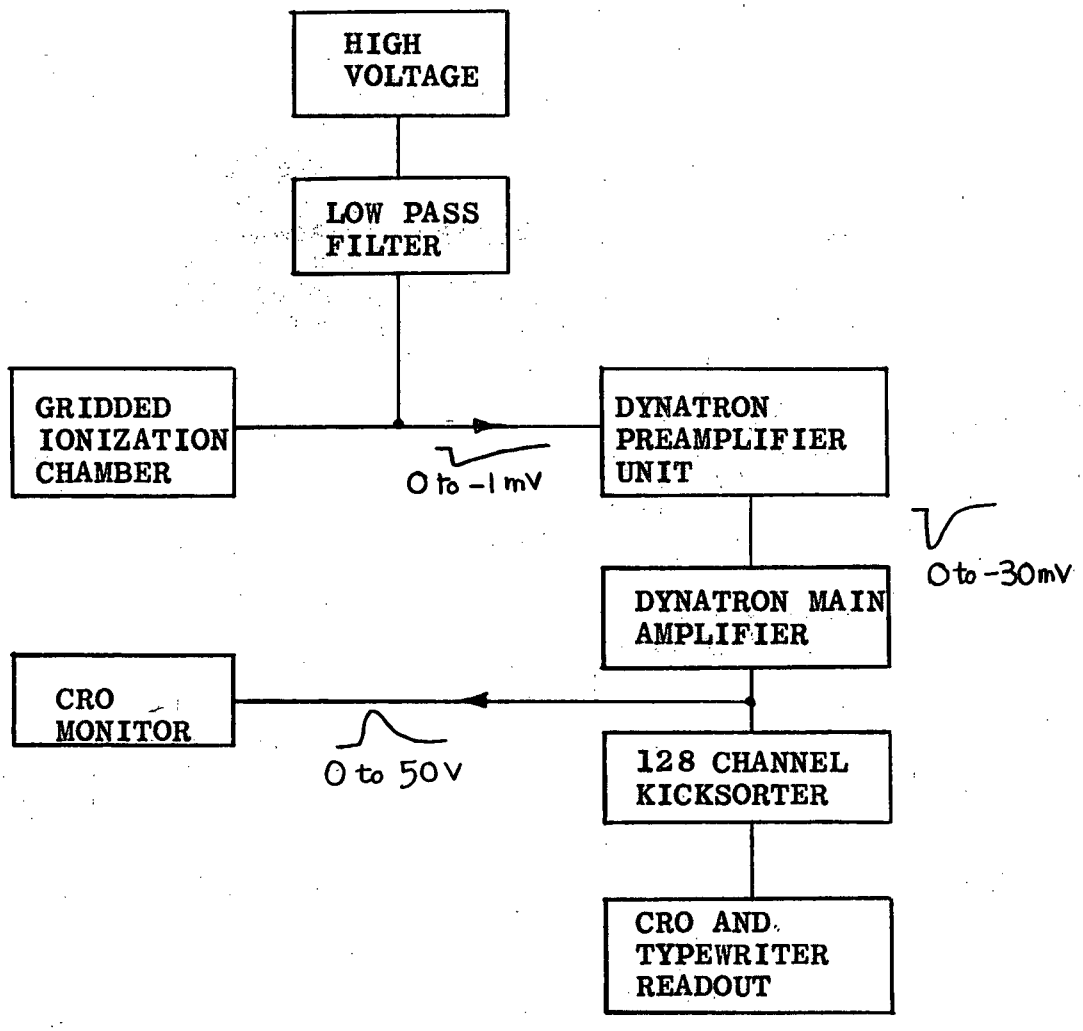

FIGURE 2 Pulse Amplification and Analysis System.

place after the first stage of amplification. Since the amplifier used provides for this, the load resistor R_3 was chosen at 10 meg. to make the time constant R_3C large compared to the chamber collection time ($\sim$ 10 μsec). C is the chamber capacitance and was estimated from the chamber geometry at 30 pf.

Some problems were encountered with noise produced by the high voltage. This noise comprised spurious pulses of similar shape and amplitude to those from the chamber. These were traced to breakdown in the filtering network. Low amplitude background "hash" was also produced by corona until the usual precautions were taken.

C. Pulse Amplification

The voltage pulses appearing at the collector of the chamber were amplified by a Dynatron Preamplifier Unit and Dynatron Main Amplifier Type 1430 A. This amplification system provides for selection from a wide range of integrating and differentiating time constants for pulse shaping. This allows for optimum signal to noise ratio and reduction of pulse pile up for given input pulse shapes. With 100 p.s.i.a. pressure in the chamber, the rise time of the pulses from the calibrating source was approximately 1.5 μsec. That associated with protons of similar energy ($\sim$ 5 Mev) was expected to be longer, and was found to be

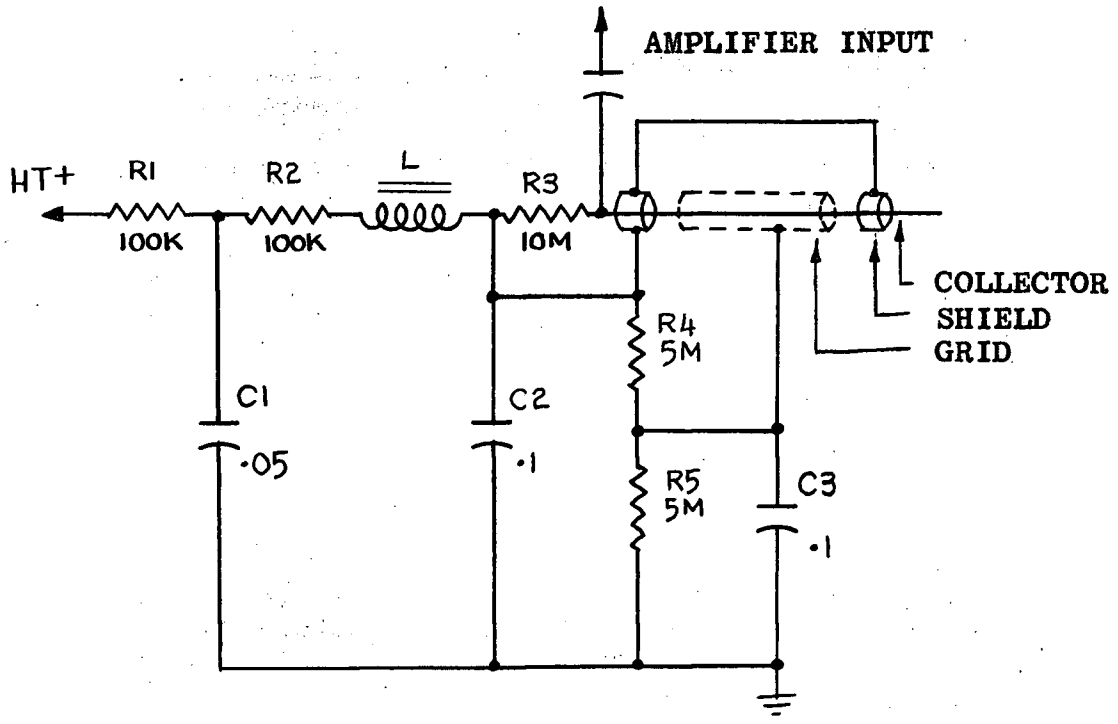

FIGURE 3 High Voltage Arrangement.

about 5 μsec. during the experiment. To avoid loss of pulse height, a differentiating time constant of 8 μsec. was chosen. In accordance with the findings of Gillespie, 1953, the integrating time constant was then also set at 8 μsec. in order to optimize the signal to noise ratio.

The Dynatron Preamplifier is a low noise, vacuum tube amplifier designed for use with nuclear counters. Because of the large amount of negative feedback incorporated in its design, the principle noise contribution from this amplifier comes from the input stage. This comprises two 6AK5 pentodes in a "cascode" configuration. It was found that the overall amplifier noise could be further reduced by replacing the first tube of the cascode by a 7586 nuvistor medium mu triode.

Because of similarity in operating conditions for the nuvistor and the 6AK5, this modification was relatively simple, and comprised a change of load resistor R_6 from 3.3K to 7.5K and introduction of a heater shunt of 150 Ω. The nuvistor was provided with a grounded, convection cooled, copper heat sink. The circuit of the modified input stage is shown in Figure 4, which uses the nomenclature of the Dynatron Manual. The use of a nuvistor as an input stage for a nucleonic amplifier is endorsed by the findings of Heywood, 1960.

With pulses of carefully regulated height (voltage) from a pulse generator supplied to the test input of the

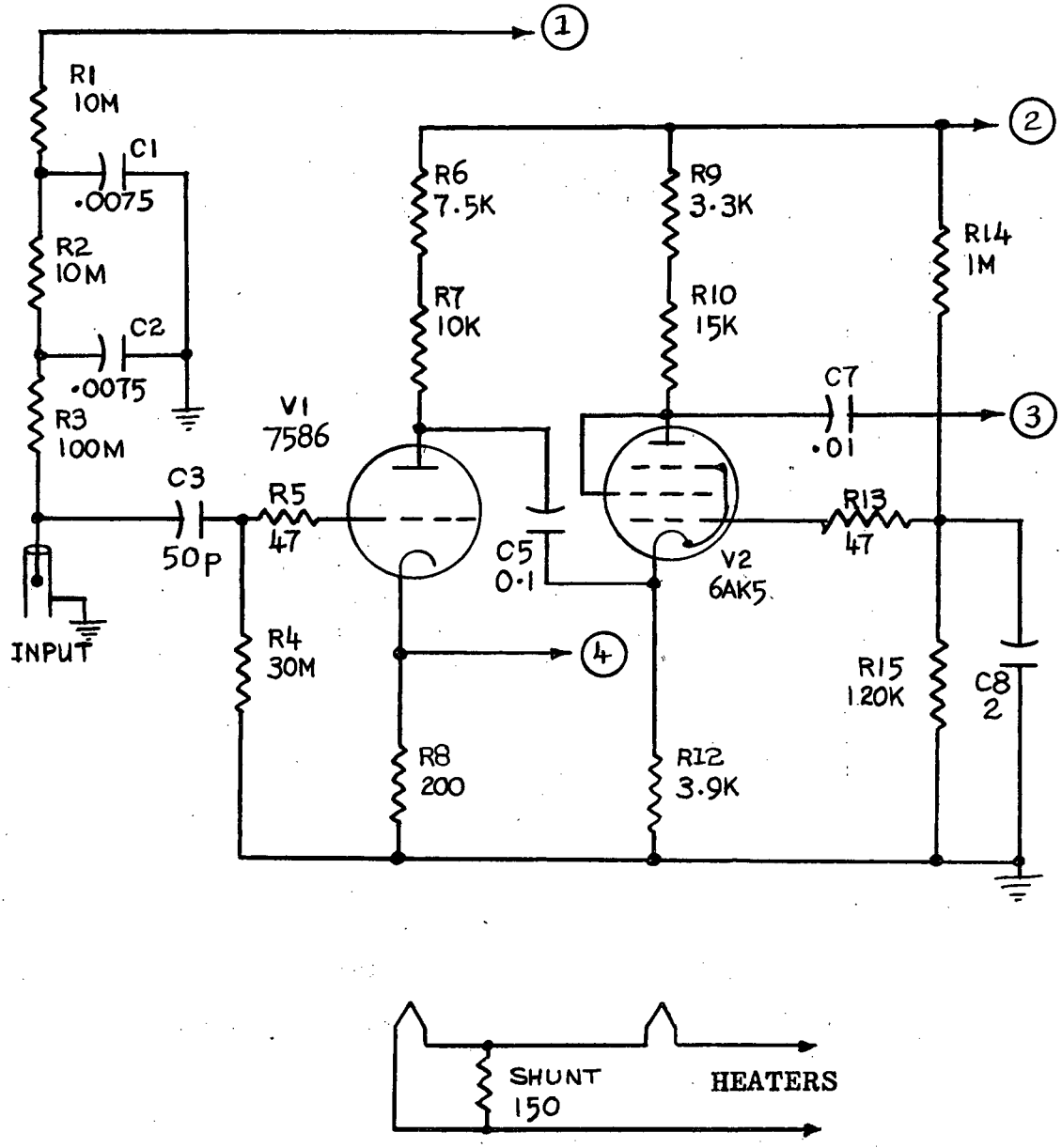

FIGURE 4 Modified Input Stage for Dynatron Head Amplifier.

(1) E.H.T. (Test input)

(2) + 250 volts

(3) to V3 input

(4) Feedback loop to R23

preamplifier, the noise introduced by the entire amplifying system as a function of the choice of input stage, was compared by monitoring the output with a 256 channel kicksorter. With the amplifier time constants and gain left at the settings determined for the experiment, the test pulse height was adjusted to fall into the same channel of the kicksorter as the peak of the pulse height spectrum from the calibrating source when the collector voltage was applied.

The noise superimposed upon the constant pulse height delivered by the pulser causes a random fluctuation in the height of the pulses seen by the kicksorter. The contour of the spectrum registered follows a Gaussian distribution whose width at half height is proportional to the r.m.s. noise voltage, and whose mean, or peak, occurs in the channel corresponding to noiselessly amplified pulses. The kicksorter resolution, taken as the ratio

$$R = \frac{\text{width of distribution (channels)} \times 100}{\text{channel number of peak}} \quad \%$$

is therefore a measure of amplifier noise for comparison purposes, and is also a measure of electronic noise contributing to broadening of peaks in the experimental spectrum. The latter is usually given in keV so that its effect can be applied directly to a pulse height spectrum involving a wide range of energies. In the present case the noise

in keV is the product of the electronic resolution and the alpha particle energy, 5.15 Mev at which energy the resolution was measured.

Several 6AK5 pentodes and two nuvistors were tried in this way. Since R is a measure of mean square noise voltage, one can estimate the intrinsic width of the pulse height spectrum from the calibrating source as follows:

$$R_\alpha^2 = R^2 - R_e^2$$

where R_α = Intrinsic resolution of source and counter

R_e = Resolution of electronics (using pulser)

R = Measured resolution of source and counter.

The results of these trials are summarized in Table 3. The trials were done with an argon pressure of 70 p.s.i.a.

TABLE 3

RESOLUTION MEASUREMENT SUMMARY

	Best 6AK5	Best 7586 Nuvistor
R_e	3.7% (190 keV)	1.5% (77 keV)
R	4.7%	3.4%
R_α	2.9%	3.0%

D. Electron Pile Up

The gamma ray flux gives rise to large numbers of energetic electrons as a result of pair production, Compton scattering and photoelectric effect in the materials constituting the chamber and its content. Fortunately the stopping power of the argon for these is small compared to that for protons, and they lose little of their energy in the sensitive volume. A relativistic electron loses approximately 16 keV per cm in argon at 100 p.s.i.a. Such an electron would lose a maximum of 400 keV in the chamber. However, if the electron flux is large, the simultaneous passage of many electrons through the gas can give large pulses similar to those expected from one heavy charged particle. ("Simultaneous" here is extended to include those sufficiently close that their respective pulses are not resolved by the amplifier.) This effect is known as electron pile up.

In the present case, the majority of the material giving rise to electrons is in the chamber walls. The pile up can therefore be reduced only by decreasing the gamma flux or by decreasing the resolving time of the amplifier. It was found, however, that the gamma flux from the target was not sufficient to produce an unacceptably high count rate over 1.5 Mev. It was found by Robertson, 1963, that the background count due to electrons drops

approximately exponentially with increasing energy. The electron background is, of course, statistical in nature and hence decreases the energy resolution of the chamber. The resolution of the system for pulses due to the calibrating source alpha particles was 3.4% (after purification) with no gamma flux and 5.5% in the presence of the flux used during the runs. The electron background was estimated by observing the effect of a natural source giving a comparable flux through the chamber, but of gammas below the photodisintegration threshold energy. This is shown in Figure 9.

CHAPTER III

GAMMA RAYS

A. Reaction for the Production of Gamma Rays

The gamma rays used in this experiment were from the reaction $Li^7(p,\gamma)Be^8$ in the neighbourhood of the 441 keV resonance. This reaction has been investigated in detail by Mainsbridge, 1960 (two papers). The pertinent results of these investigations are as follows.

(a) Gamma ray energies: two gamma rays are produced with energies 17.27 and 14.3 Mev plus $^7/_8$ of the incident proton energy. At the 441 keV resonance these correspond to 17.64 and 14.7 Mev respectively. The ratio of intensities has a peak value of 2.3 at resonance, in favour of the 17.6 Mev radiation. The ratio drops to unity at bombarding proton energies of approximately 380 keV and 580 keV. The line width of the 17.6 Mev gamma ray is 12.2 keV, and that of the 14.7 Mev one of the order of 2 Mev. The cross section for the reaction is 6 mb. at resonance.

(b) Angular distribution: the gamma yield is isotropic within 6% at resonance.

B. Production of the Target

The lithium target was made in the target chamber illustrated in Figure 5. Approximately 100 watts of a.c. power were delivered to the furnace at 15 volts, through a Variac transformer. This was sufficient to heat it to red heat in just under one minute. At this temperature a 40 keV thick target could be deposited in a few minutes.

The copper target backing was highly polished, meticulously cleaned and clamped into the water cooled copper target holder, which could be moved via a vacuum seal to shift the target from the furnace tube to the beam tube.

Approximately a tenth of a cubic centimeter of natural lithium metal was scraped clean under benzene and allowed to outgas under vacuum in the furnace with about 10 watts applied to the heater, for one hour. The full 100 watts were then applied with the back of the target holder exposed to the furnace tube. After the furnace attained red heat a black deposit appeared on the copper. When this began to turn white, the frame was rotated to expose the prospective target to the furnace. A fairly substantial white deposit obtained in 2 - 3 minutes amounted to a satisfactory target, 20 - 40 keV thick.

The excitation function of the target used for the final run recorded here appears as Figure 6. This target

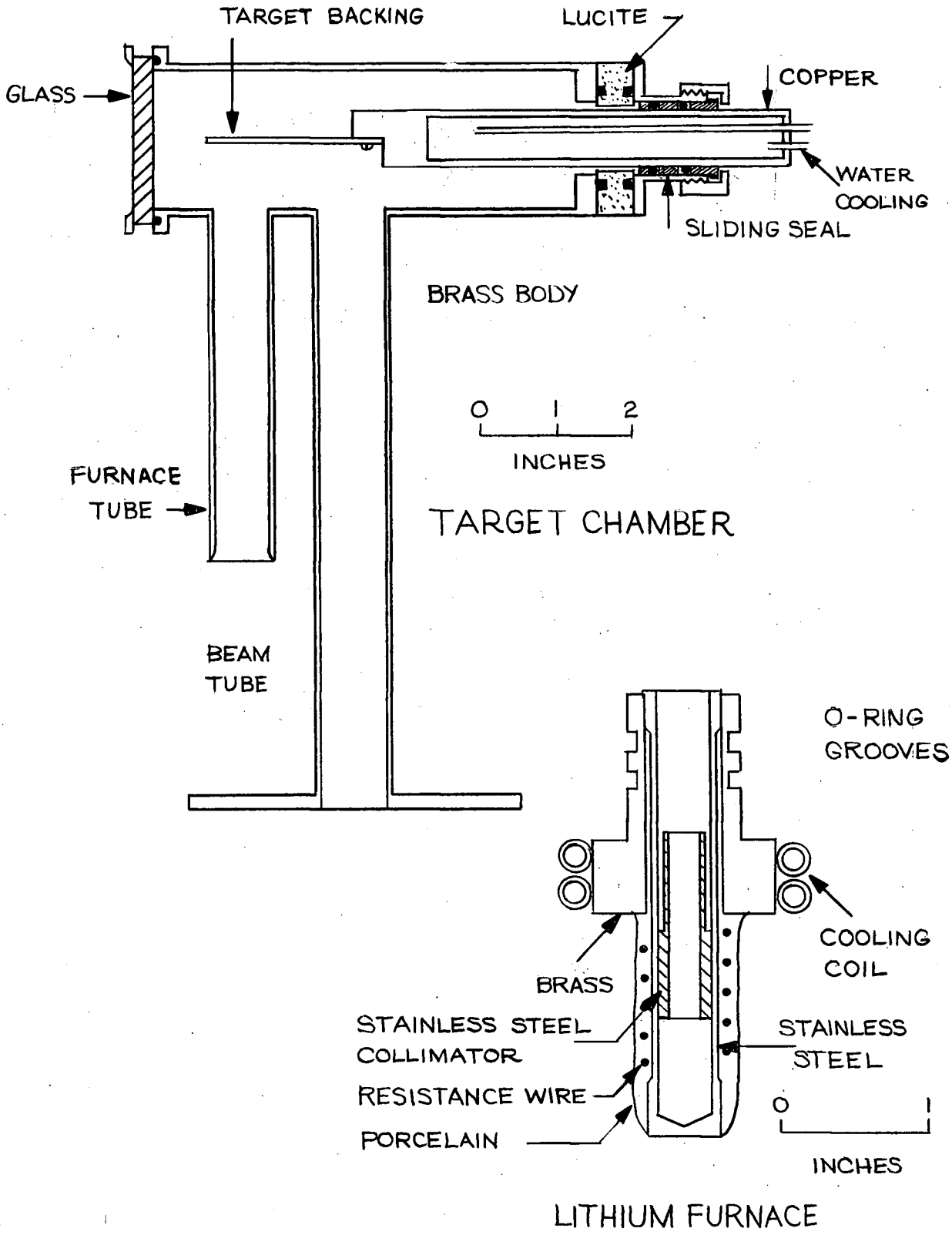

FIGURE 5 Lithium Target Chamber.

was 23 keV thick and lasted for 8 hours with a proton current of 15 μamps before the yield was reduced below a useful level by flaking. The initial yield was approximately 40% of the theoretical target yield of 9,200 gammas per steradian per microcoulomb calculated from the excitation function shown in Figure 6. The low experimental yield is attributed to oxide contamination of the target.

C. Measurement of Gamma Flux

The integrated gamma flux was measured with a $2^{3}/4$ inch diameter by $4^{1}/2$ inch long NaI(Tl) scintillation counter. This was placed 82 centimeters from the target at an angle of 133° ± 2° to the direction of the proton beam.

The counter was the same one used by Robertson, 1963, and the counting and calibrating procedures were identical to his, using the same amplifier and scaler. In this case the upper and lower level discriminators were set to pass pulses corresponding to gamma rays of energy between 8.8 and 19 Mev. The uncertainty in the number of gamma rays counted due to determination and stability of the lower level discriminator bias was ± 0.7%.

The energy spectra of the gamma rays from the lithium target and from the RaTh calibrating source were obtained by feeding the amplifier output into the 256 channel kick-sorter. These spectra are shown in Figure 7. The linearity

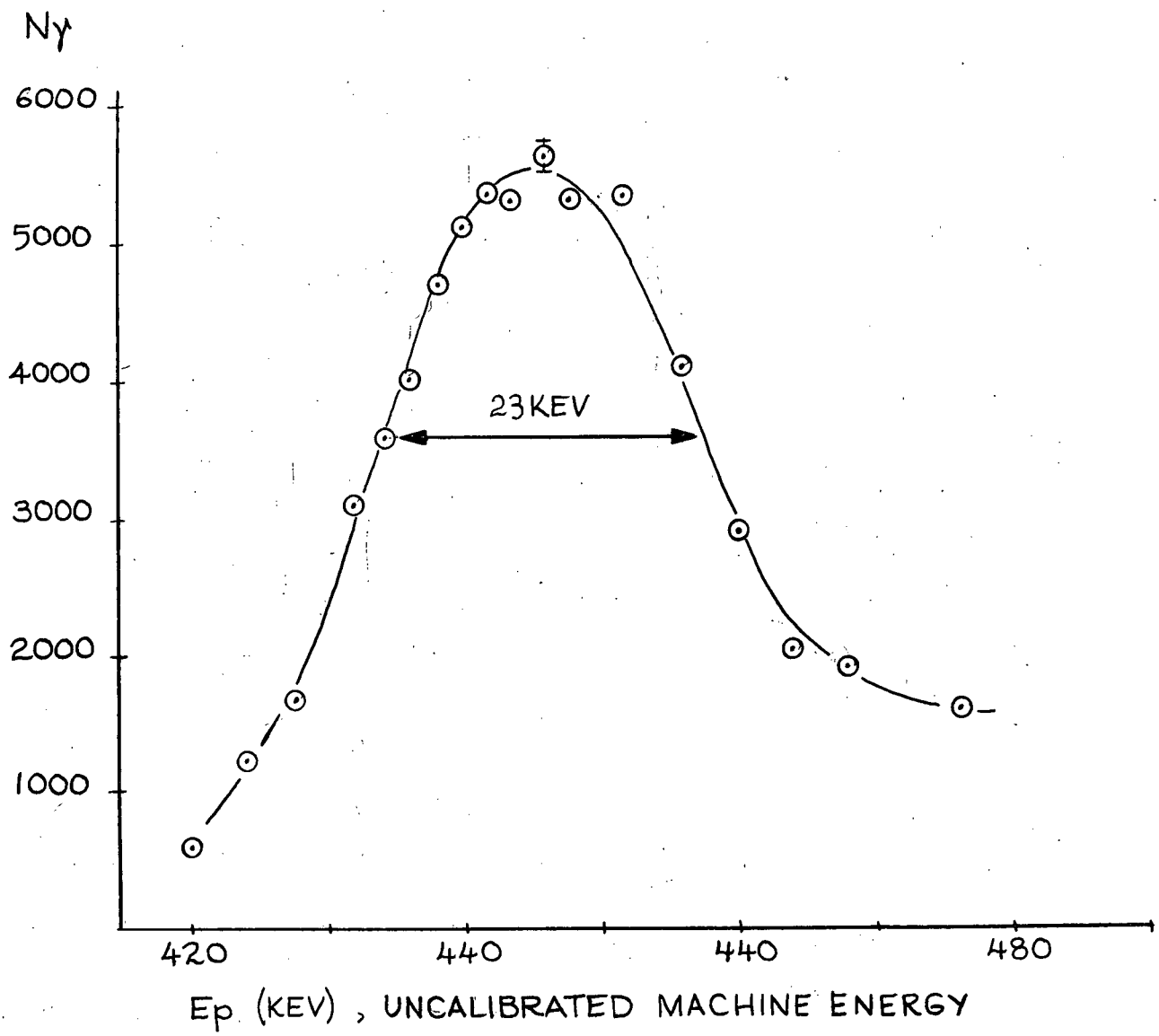

FIGURE 6 Lithium Target Excitation Function.

of the kicksorter was checked using a pulse generator (Robertson, 1957). It was thus possible to introduce a correction to the number of gamma counts due to the error in the setting of the lower level discriminator.

The efficiency of this gamma counter has been measured by Singh, 1959, up to 12.1 Mev. He also calculated theoretical values which are in good agreement with experiment for the three crystals he used. The curve of efficiency for half energy bias as a function of gamma ray energy for the crystal used in this work was seen to be approximately linear from 6 to 12 Mev. This curve was then extrapolated up to 20 Mev without theoretical contradiction. A point at 20.3 Mev was obtained by intercomparison with a standard, thick walled brass geiger counter whose efficiency was also being measured, (Morrow, 1958). The efficiency curve of the geiger counter was predicted to be linear from a few Mev up to at least 20 Mev. This also was found to be in good agreement with experiment. While agreement of the flux measurement at the 20.3 Mev energy between the two types of counter is a good indication of the validity of the extrapolated efficiencies, it is not an absolute measurement, and the possibility of an error of the order of 10% must be accepted. The value of the efficiency of the counter according to the semiempirical determination discussed above varies linearly from 80% at 14 Mev to 81.5% at 20 Mev. A value of 81% was therefore used in this work.

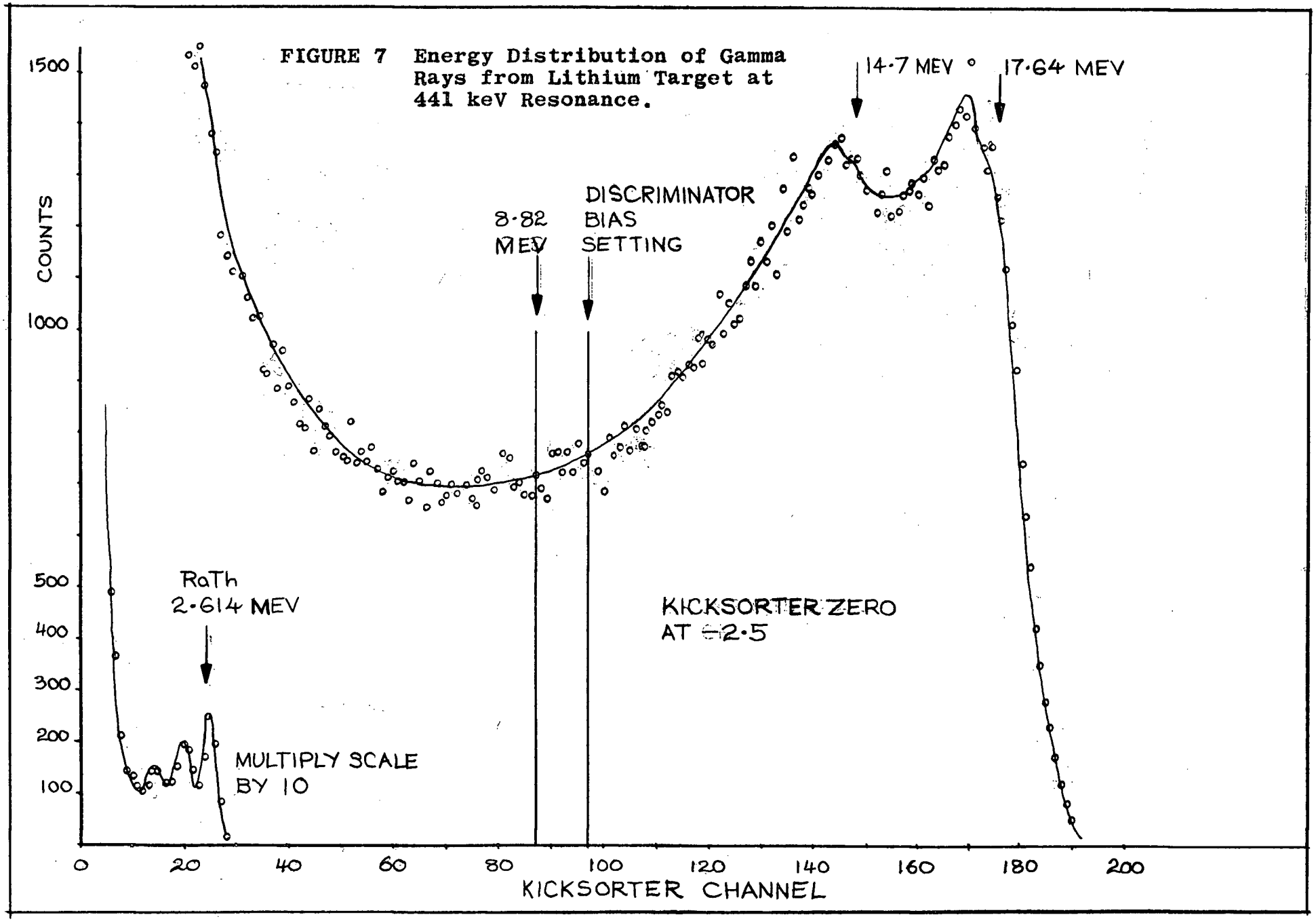
FIGURE 7 Energy Distribution of Gamma Rays from Lithium Target at 441 keV Resonance.
14·7 MEV
17·64 MEV
8·82 MEV
DISCRIMINATOR BIAS SETTING
RaTh 2·614 MEV
MULTIPLY SCALE BY 10
KICKSORTER ZERO AT −2·5
COUNTS
1500
1000
500
400
300
200
100
0
20
40
60
80
100
120
140
160
180
200
KICKSORTER CHANNEL

CHAPTER IV

THE PROBLEM OF CHAMBER BACKGROUND

As stated in the reports of Hay and Warren, 1959, and Monier, 1960, after whose work the gridded ionization chamber became available for the present experiment, the interior of the chamber was coated with graphite. This is a common practice for reducing background due to the natural alpha activity from the inevitable impurities in commercially available metals. When the chamber was overhauled and re-activated after its two year rest, the background was found to be excessively high, and displayed peaks in its energy spectrum at 5.7, 6.1 and 7.9 Mev. These were well resolved, and were attributed to some alpha emitting contamination.

The chamber was then completely cleaned and fresh graphite applied in the form of aquadag. The background was then found to be satisfactory and devoid of noticable peaks. This situation did not persist, however, as an unacceptable background was again found to be present at the time when a preliminary run was made on the photodis-integration. This was the more interesting because the background was reduced to its original low level when the gas was replaced.

It was suspected that the graphite used might have been contaminated by an active nuclide having radon as a daughter product. The short half life of the radon isotopes would account for the rise in background within a moderate time, and its gaseous nature would account for the reduction with the change of gas.

A considerable amount of attention has been devoted to the problem of background in gridded ionization chambers in this laboratory, due to the current experiments on the photo-disintegration of helium 3 (Robertson, 1963). This experiment is particularly sensitive to chamber background because of the low count rate expected as a result of the small cross section. In anticipation of progressing the helium 3 experiment beyond the work of Robertson, MacDonald and Healy of this laboratory have developed a technique for reducing the background contribution from the chamber walls well below that found possible with graphite lining.

Their technique (MacDonald and Healy, private communication) involved lining their chamber with a polyester film produced by du Pont under the trade name "Mylar". This is a tough, clear plastic with a low vapour pressure, composed of 62.5% carbon, 4.2% hydrogen and 33.3% oxygen. The thickness used was 3.63 (10^{-3}) cm, corresponding to 5.0 mg/cm^2, which is sufficient to stop a 7 Mev alpha particle. In order to render the inner surface conducting so that it could be maintained at ground potential and not

distort the field within the chamber, the Mylar was coated with a very light film of gold, evaporated on under vacuum. A thickness of gold giving a resistance of the order of a few thousand ohms per inch was deemed adequate. Such a film was quite transparent in appearance, and considered unlikely to contribute heavily to the background from its natural impurities.

Because of the success of this technique in reducing the background in the helium 3 chamber, it was decided to employ it for the argon chamber in place of the graphite. Incorporation of the Mylar indeed reduced the background by a factor three over the best graphite value, giving of the order of 30 counts per hour with energy greater than 2 Mev. Divided by the wall area surrounding the active volume this amounts to better than 0.03 counts per cm^2 per hour. This compares favourably with the figure .07 quoted for aquadag by Sharpe, 1955.

This background remained constant and devoid of peaks within statistical fluctuations, for an observation period of two days. The photodisintegration was then progressed, only to find just before the run that it had risen again, and in fact showed peaks as before. The fact that the gas purifying calcium-magnesium eutectic had been inserted after the satisfactory background observation, led to the conclusion that this must be responsible. Again the background was observed to increase with time, and again it could be

restored to its original value by replacing the gas. A sharp increase of the background was noted after a brief heating of the purifier. The indicated conclusion that an isotope of radon was being produced in and diffusing from the eutectic was later corroborated by obtaining a positive indication on a tritium monitor from a sample of the eutectic stored for some days in a plastic bag.

A fresh batch of eutectic was then tried with somewhat better results. Some contamination was still present, because the background became significant after approximately three days. For the first two days after filling the background was considered low enough to conduct the experiment. The runs yielding the results reported on here were all done within 24 hours of filling the chamber, and the background is practically negligible. The background after the runs were completed was monitored for two hours and normalized to the running time for the purpose of subtraction from the experimental result. This is shown in Figure 8, and averaged close to 60 counts per hour.

The precise nature of the contaminant was the subject of some speculation. Of the three isotopes of radon occuring in the natural radioactive series, Rn^{222} is the most obvious choice. Beginning with Ra^{226} in the Uranium Series, the decay scheme involved is given in Table 4. It can be seen from the table that the alpha energies involved

are in agreement with the positions of the peaks in the background energy spectrum within 200 keV. No such agreement is even approximated by the decay schemes of the other natural radon isotopes.

TABLE 4

DECAY SCHEME FOR RADON^{222}

NUCLIDE	HALF-LIFE	TYPE OF DECAY	PARTICLE ENERGY (MEV)	BACKGROUND PEAK (MEV)
Ra^{226}	1620 y	α (100%)	4.78 max	
Rn^{222}	3.82 d	α (100%)	5.49	5.7
Po^{218}	3.05 m	α (99%)	6.00	6.1
Pb^{214}	26.8 m	β (100%)	0.7	
Bi^{214}	19.7 m	β (99%)	3.17	
Po^{214}	$1.6(10^{-4})$ s	α (100%)	7.68	7.9
Pb^{210}	22 y	β (100%)	0.02	

The energy spectrum of the background in which the peaks were identified was made within a week of filling the chamber. Owing to the 3.8 d. half-life of the radon one would not expect secular equilibrium to have been approximated in this time. The relative numbers of counts in the three peaks were in agreement with this supposition (5.7 Mev, 320; 6.1 Mev, 150; 7.9 Mev, 85).

CHAPTER V

EXPERIMENTAL RESULTS

The results upon which this report are based are shown in Figure 8. This shows the energy distribution spectrum of charged particles losing energy in the chamber, with an argon pressure of 103 p.s.i. absolute, in approximately 8 hours of running time with a single lithium target. The reproducibility of this result is confirmed by comparison with two independent runs done earlier with different targets and different fillings of argon. The spectra are essentially the same, although the earlier runs were of poorer energy resolution and had the gain set so that particle energies up to 11 Mev could have been registered.

Figure 8 was plotted as the sum of three individual runs with the kicksorter rezeroed before each one. These runs, when individually plotted, exhibited the same characteristics as their sum. The plots were made from the digital, typewritten output of the kicksorter.

It was concluded from Table I that the charged particles contributing to the observed results could only have been protons and alpha particles.

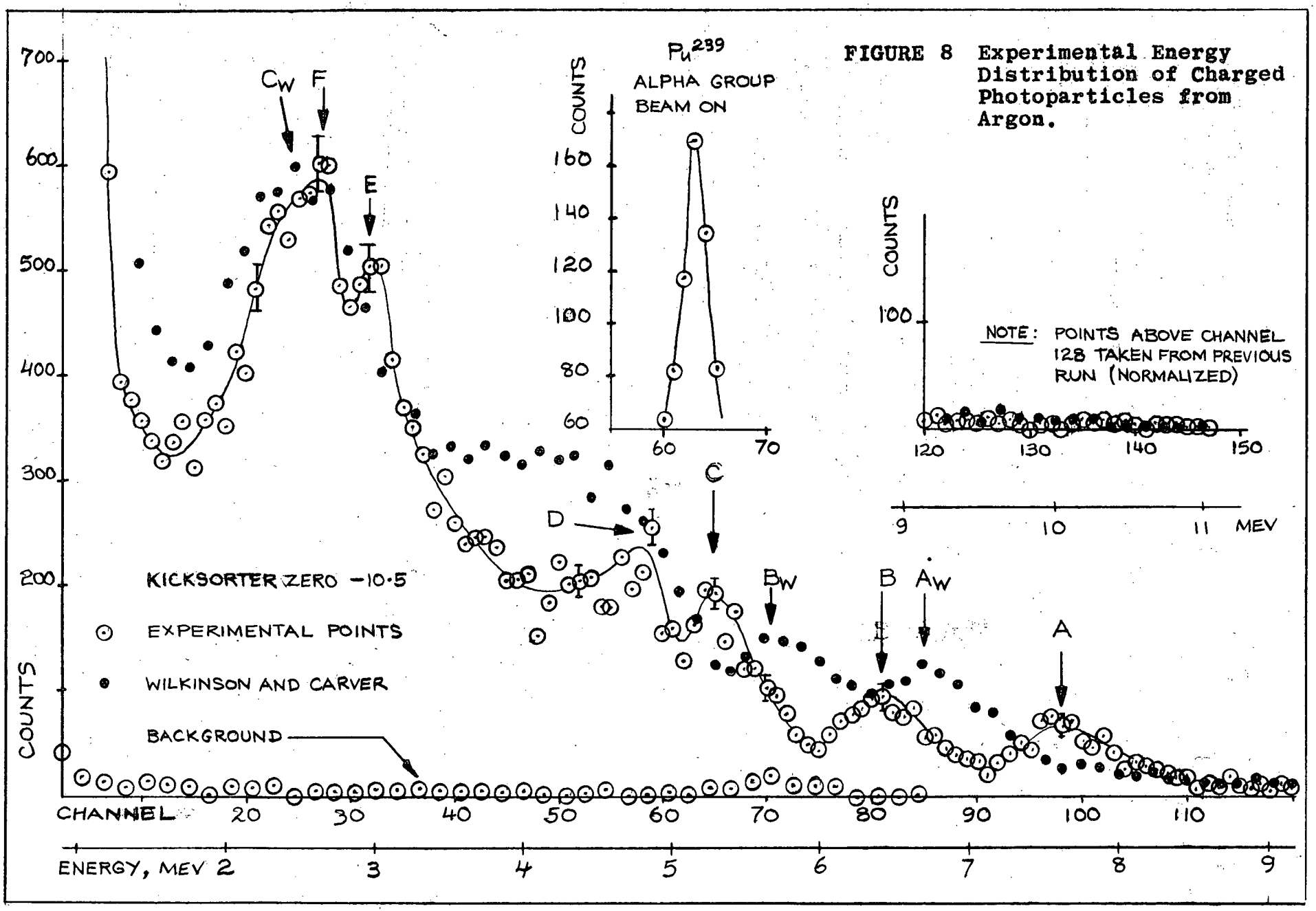

FIGURE 8 Experimental Energy Distribution of Charged Photoparticles from Argon.

A. General Description

Figure 8. shows the experimental energy distribution with both kicksorter channel numbers and energy released in the chamber as abscissae. The energy scale was set by the calibrating source, whose spectrum is shown on the diagram as an inset. This peak corresponds to 5.15 Mev alpha particles from Pu^{239}, and was registered in the presence of the gamma flux used for the experiment. The linearity of the kicksorter was checked using the pulse generator at various pulse voltages as an input. The kicksorter zero was determined to be at channel -10.5 by extrapolation.

The experimental points published by Wilkinson and Carver, 1951, are shown for comparison. The points are plotted at the energies shown in the publication, with the vertical scale (number of counts per point) normalized so that the height of the peak at 2.5 Mev is the same as that shown for the present work.

It is immediately apparent that the present results are in accord with the main features of those given by Wilkinson and Carver. The main differences are in the energy scale and in the resolution obtained. In Figure 8 features of the earlier work are indicated by letters with the suffix w. Peaks Aw and Bw are spaced the same as A and B but are given at an energy 0.8 Mev lower. The

correspondence is good with respect to peak shape and relative number of counts. Peaks C and D were not resolved by Wilkinson and Carver, and, allowing for the energy scale discrepancy, are represented by their plateau from 3.5 to 4.5 Mev. The peaks F and Cw clearly correspond, and while there is one point which might indicate the presence of a peak corresponding to E, this was not inferred in the earlier work. The discrepancy in the energy scales is approximately 11%.

An attempt has been made to resolve the experimental energy distribution of Figure 8 into peaks representing individual contributions. These are shown as broken lines in Figure 9, under the distribution after subtraction of the chamber background. The estimated electron background (see Chapter II) is also shown.

Because of the 2 Mev width of the 14.7 Mev contribution to the gamma flux, it is not expected to see any well defined peaks due to events stimulated by this radiation. Furthermore, such events are expected to be fewer than those originating through 17.64 Mev gammas, for two reasons. Firstly, because of the ratio of intensities (see Chaper III) and secondly, because the lower energy is further removed from the maximum of the giant resonance in the absorbtion cross section. The effect of the latter on the photoproton yield can be inferred from the results of McPherson et al, 1954.

FIGURE 9 Partially Analyzed Energy Distribution of Charge Photoparticles.

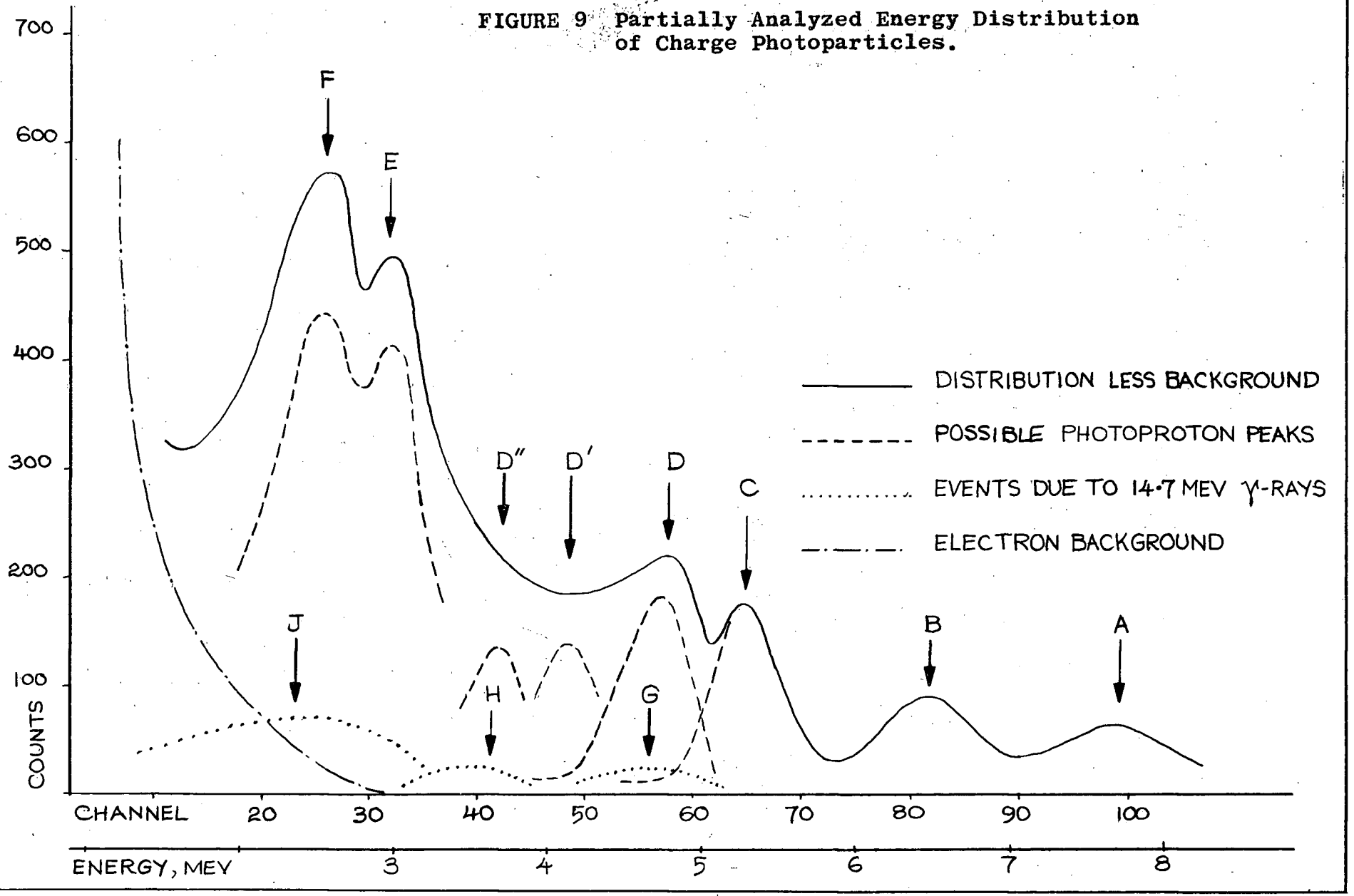

According to their curve showing the photoproton cross section of argon as a function of gamma energy, the cross section at 14.7 Mev is approximately 1/3 of that at 17.6 Mev. In view of these considerations, one could expect a maximum of 1/6 of the total number of counts observed to be due to the 14.7 Mev radiation.

The peaks A and B were assumed to be due to the (γ,α) reaction because they represent charged particle energies well above those allowed for protons by the listed Q-value. The wall effect for these peaks was therefore considered negligible (see Table 5). Although the peaks are rather wider than expected for alpha particles, they are still narrower than anticipated for any events initiated by the 14.7 Mev gammas. It is therefore assumed that A and B are due to the 17.6 Mev radiation. This assumption is supported by the absence of any peaks at higher energy.. Events resulting from 14.7 Mev gammas leading to the same states of the residual nucleus as those inferred from peaks A and B might therefore be evident in the distribution at energies 2.9 Mev lower than A and B. Peaks G and H have been postulated on this basis, and represent approximately 1/6 of the number of counts in A and B. For this purpose it was assumed that the photoalpha cross section dependence upon photon energy would be similar to that for photoprotons. This is expected because the energy dependence

is characteristic of the giant absorbtion resonance, which is independent of the decay channel.

Peaks C and D were associated with photoprotons leaving the residual nucleus Cl^{39} in its ground and first excited state respectively. C was drawn in with the shape of its low energy side as suggested by that of the calibrating source peak. It is expected that the experimental peaks be somewhat broader than the calibrating source peak because of random track orientation in the former case. This is particularly true for proton peaks because of the greater track length involved. The number of counts in peak C was obtained by direct summation, by channels, from the plot. This number was then used to calculate the wall effect as per Appendix B, and the low energy tail of the peak was modified accordingly. Peak D was drawn in after C and G were subtracted from the distribution. The fact that it requires G to reduce D to the same height as C supports the existance of G, because one does not expect D to contain more counts than C due to the increasing effect of the Coulomb barrier with lower energy. The wall effect was computed for D in the same way as for C.

The decomposition of the remainder of the distribution is of a somewhat speculative nature because the contribution due to the 14.7 Mev radiation can only be estimated very roughly as outlined above. Since the Q-value does not allow

formation of the residual nucleus Cl^{39} in any but the lowest lying excited states, it is assumed that the $^1/_6$ of the photoproton events observed which can be attributed to the 14.7 Mev gammas results in the group J, occurring approximately 2.9 Mev below peaks C and D. Because of the influence of the Coulomb barrier, the peak J is shown favouring higher energy protons.

The general shape of the remaining part of the distribution has the appearance predicted by the statistical model, as shown, for instance, by Spicer, 1955. The fact that some structure (peak E) is apparent indicates that the level density at the corresponding excitation of the residual nucleus is not very great, or at least that there is a gap between two groups of levels at the excitation energy corresponding to the dip in the distribution between peaks E and F. The high energy tail requires a minimum of two levels to account for it, such as indicated by D' and D" in Figure 9. The remainder would require of the order of 10 levels with spacing of approximately 200 keV, depending largely on the rate of decrease of photoproton cross section as a function of exit channel energy, due to the Coulomb barrier. The resolved peaks together with their energies as obtained from the alpha calibration, the number of counts in each, and the appropriate wall effect corrections obtained by the method of Appendix B, are given in Table 5.

TABLE 5

EXPERIMENTAL RESULTS

PEAK	ENERGY (MEV)	N_o	N	N(E)/ CHANNEL	REACTION ASSIGNMENT
A	7.60	850	915	0.6	$A^{40}(\gamma,\alpha)S^{36}$?
B	6.44	900	960	0.7	$A^{40}(\gamma,\alpha)S^{36}$?
C	5.25	1370	2500	15.0	$A^{40}(\gamma,p)Cl^{39}$
D	4.72	1370	2300	13.8	$A^{40}(\gamma,p)Cl^{39}$
E	2.9	10335	13950	83.8	$A^{40}(\gamma,p)Cl^{39}$
F	2.5				$A^{40}(\gamma,p)Cl^{39}$

N_o = number of counts in the peak

N = number of counts corrected for wall effect

N(E)/Channel= number of counts per channel expected in the low energy tail due to wall effect.

B. Discussion

The identification of peaks C and D with proton events leading to the ground and first excited states in Cl^{39} gives good agreement with the Q-values quoted for the $A^{40}(\gamma,p)Cl^{39}$ reaction. Peak C implies a Q-value of -12.39 Mev. The peak D puts the first excited state of Cl^{39} at 0.53 Mev. The energy level diagram for Cl^{39} given by Endt and and der Leun, 1962, Appendix D, indicates the presence of levels at 0.36 and 0.8 Mev. Peak D, therefore, could be the unresolved combination of events leading to both of these. The lack of resolution in that case could be due to the presence of peak G.

The postulation of further energy levels based on the group including D', D", E and F would not be meaningful without considerably better energy resolution. That the group is due to photoprotons rather than photoalphas as suggested by Emma et al, 1959, is required by the large photoproton cross section measured by workers using the residual activity of Cl^{39} as evidence.

The assumption that peaks A and B are due to the photoalpha process from the 17.6 Mev radiation requires an explanation for the absence of alpha groups at higher energy as might be expected from the Q-values given in Table 1. From the Q-value of Everling et al, 1960, one

expects alpha particles leaving S^{36} in its ground state to form a group at 10.8 Mev, but no trace of this was found. Possible explanations are the existance of an isotopic spin or other selection rule, or a large error in the Q-value.

Because the ground states of both A^{40} and S^{36} are $T = 2$, $T_z = 2$ states, there is no obvious isotopic spin selection rule. $\triangle T = 0$ for alpha emission, and $\triangle T = 0$ is allowed for electric dipole gamma absorbtion in this case. Since both ground states have $J = 0$ and electric dipole absorbtion requires $\triangle J = 1$, the alphas would have to be emitted with $\ell = 1$. Such a p-wave transition is less favoured than s-wave transitions, but it is not forbidden.

If the peak A is taken as representing the transition to the ground state of S^{36}, a Q-value for the reaction $A^{40}(\gamma,\alpha)S^{36}$ of -10.0 Mev is implied, inferring that the nuclidic mass of S^{36} is 3.2 Mev greater than given by Everling et al, 1960. Such an assumption has the consequence that the decay by electron capture of the ground state of Cl^{36} leading to S^{36} is energetically forbidden, contrary to the findings of Drever and Moljk, 1955. Alternatively, the mass of S^{36} might be 1 Mev or more smaller than the value given by Everling et al, in which case the peak representing the transition to the S^{36} ground state would

have been off the kicksorter scale.

Various other possibilities were considered to account for peaks A and B. Reactions involving the materials of the chamber are virtually eliminated both by the shape of the peaks and by the fact that they were seen, with the same relative number of counts, by Wilkinson and Carver. The reactions $A^{36}(\gamma,p)Cl^{35}$ and $A^{36}(\gamma,\alpha)S^{32}$ cannot be ruled out, but the Q-values involved both indicate that peaks should occur at higher energy. Also, in order to account for a peak the size of A or B, the cross section would have to be at least two orders of magnitude greater than for the corresponding events involving A^{40}, because of the very low concentration of the lighter isotope.

Any second order reactions must also be excluded because of the relatively large cross section represented by peaks A and B. There remains the possibility of neutron induced reactions. Neutron production in the target should have been excluded by the negative Q-values involved. This was checked upon, using a BF_3 long neutron counter to look for differences in neutron flux as the target was moved in and out of the proton beam. With the target "out" the beam was incident upon the copper target backing next to the target. A run of half an hour was done with the beam on the copper backing, and the number of counts from the chamber representing energies above 5 Mev were negligible. No significant difference in neutron flux was seen when the

target was in position. A considerably longer run was done using the mass two beam at a bombarding energy of 880 keV. The energy spectrum of charged particle events in the chamber showed a count rate several times higher than expected from the monitored gamma flux. The difference was attributed to neutrons arising from the deuterium present in the beam, and showed a broad peak between 2 and 3 Mev, but with no significant contribution above 5 Mev.

C. The Cross Section

The calculation of the total and partial cross sections has been relegated to Appendix C. The total cross section for the photoproduction of charged particles by lithium gamma rays was 5.8 mb. Based on the assignments made above, this was resolved into a photoproton cross section of 5.2 mb and a phtoalpha cross section of 0.6 mb. The values obtained for these cross sections could be in error by as much as 10% due to the uncertainty in the gamma ray monitoring.

D. Conclusion

Apart from improved resolution and an 11% discrepancy in the energy scales, the present results are in good agreement with those of Wilkinson and Carver, 1951, both in shape of the energy distribution and in the measured cross section.

The interpretation is different from theirs because of the more accurate Q-values now available as a guide. These results do not admit a photoproton cross section as high as those found by McPherson et al, 1954, and Spicer, 1955.

In order to arrive at more certain conclusion as to the nature of peaks A and B in the present spectrum further experimental evidence would be helpful. It would be particularly useful if alpha and proton events could be distinguished. Since alpha tracks are much shorter than proton tracks, the simplest method would be to repeat the experiment at lower gas pressure, such that the wall effect for proton events becomes very large. If the indications of such a run are inconclusive, more sophisticated means could be employed such as use of solid state counters with alpha absorbing films.

It would also be useful to obtain a spectrum including peaks C, D, E, and F with better energy and kicksorter resolution. Better energy resolution might be obtained by reducing the gas pressure to, say, 80 p.s.i.a., where wall effect and yield would still be reasonable. By this expedient it might be possible to obtain a better indication of the structure of the spectrum between peaks D and E, and to resolve peak D into two components corresponding to the suspected levels in Cl^{39}.

Confirmation of the extent to which the 14.7 Mev gamma ray is effective in producing photoparticles could be obtained by conducting the experiment with a different gamma source.

APPENDIX A

Reprinted from THE PHYSICAL REVIEW, Vol. 83, No. 2, 466, July 15, 1951
Printed in U. S. A.

Photoprotons from Argon under the Action of Gamma-Rays of 17.6 Mev

D. H. WILKINSON AND J. H. CARVER*
Cavendish Laboratory, Cambridge, England
(Received May 28, 1951)

SINCE the discovery by Hirzel and Wäffler[1] of the anomalously large (γ, p) cross sections in many elements there has been much speculation as to the mechanism of the interaction of high energy gamma-rays with nuclei. Two theories have been put forward to explain the large cross section. In one[2] the individual level properties are chosen to vary in such a way as to favor the emission of high energy particles while retaining the idea of the initial formation of a compound nucleus: in the other,[3] the process is imagined as a surface photoelectric effect in which a proton lying near the surface of the nucleus is simply ejected on absorbing a gamma-quantum, no compound nucleus being formed in the ordinary sense.

We have sought to elucidate the mechanism of this interaction by determining the energy distribution of the photoprotons ejected from A^{40} by gamma-rays of 17.6 Mev produced in the reaction $Li^7(p, \gamma)Be^8$. Argon at 11 atmospheres was contained in a carbon-lined proportional counter of sensitive volume 1220 cc. The energy distribution of the photoprotons is shown in Fig. 1; the analysis was made with a ninety-nine-channel kicksorter.[4] A very weak polonium source within the counter provided the energy scale. We made irradiations at various proton energies from 450 to 1150 kev, over which range the relative proportion of 14.8- to 17.6-Mev lines increases by 3:1.[5] There was no detectable change in the distribution; this must be due almost entirely to the 17.6-Mev line.

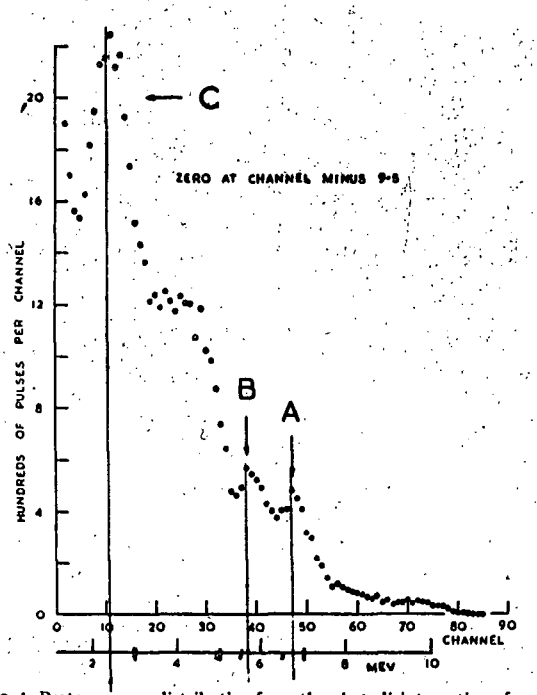

FIG. 1. Proton energy distribution from the photodisintegration of argon. (This is the experimental distribution, which must suffer a small correction for the wall-effect. The rise at low energy is due to electron build-ups.)

The tail above group A is probably due to the reaction $A^{40}(\gamma, \alpha)S^{36}$. These alpha-particles would contribute little in the bulk of the distribution owing to the relatively great importance of the barrier at lower energies and can probably be ignored.

It is immediately apparent that the bulk of the disintegration cannot be the result of a surface photoelectric effect, as this would give the main group at high energy. Group A we identify with the ground state transition: if it were due to a surface effect, it would be difficult to understand the strength of group B, which has about the right spacing from A to correspond to the first excited state in Cl^{39}.

It is also difficult to adopt the suggestion of Schiff[2] that high energies are favored, as the peak C lies at an even lower energy than would be expected on a model using an exponentially increasing level density of characteristic temperature 1 Mev such as seems appropriate from the work of Gugelot.[6] Using correct coulomb wave functions[7] through $l=5$ we have computed the expected distribution, which has a maximum at 3.0 Mev, and an intensity ratio of 7.7:1 from peak to 7 Mev. (This procedure must be rather crude for argon.) The same model predicts a ratio of 25 between (γ, n) and (γ, p) cross sections (neglecting all differences but the barrier). We may infer a (γ, n) cross section of about 15 mb:[8] our (γ, p) cross section is 5.4 mb. So the difficulty of the cross-section ratio remains without any apparent possibility of explanation by the two methods so far suggested. The answer may lie in a drastic modification of the shape of the barrier—a great change in the nuclear radius cannot be permitted.

A fuller discussion and other results will be published later.

* Australian National University Scholar.
[1] O. Hirzel and H. Wäffler, Helv. Phys. Acta. 20, 373 (1947).
[2] L. I. Schiff, Phys. Rev. 73, 1311 (1948).
[3] E. D. Courant, Phys. Rev. 74, 1226 (1948); see also J. S. Levinger and H. A. Bethe, Phys. Rev. 78, 115 (1950); and L. Marquez, Phys. Rev. 81, 897 (1951).
[4] D. H. Wilkinson, Proc. Cambridge Phil. Soc. 46, 508 (1950).
[5] R. L. Walker and B. D. McDaniel, Phys. Rev. 74, 315 (1948).
[6] P. C. Gugelot, Phys. Rev. 81, 51 (1951).
[7] Bloch, Hull, Broyles, Bouricius, Freeman, and Breit, Phys. Rev. 80, 553 (1950). We are indebted to Mr. A. M. Lane for a discussion of these functions.
[8] McDaniel, Walker, and Stearns, Phys. Rev. 80, 807 (1950).

APPENDIX B

CALCULATION OF THE WALL EFFECT

The wall effect in an ionization chamber is a combination of two types of event. Most important in their effect are events where a charged particle leaves the sensitive volume of the chamber before it has lost all its energy. This can happen as a result of collision with the chamber walls, or as a result of exit into the insensitive regions at the ends of the chamber. Of secondary importance are events where charged particles produced outside the sensitive volume enter it and lose part of their energy inside the sensitive volume.

The derivation of wall effect functions has been treated in detail by Robertson, 1963, for cylindrical chambers in terms of the following parameters:

$P(R)$ = Probability that particle hits wall or leaves sensitive volume

R = Range of particle being considered

b = Radius of the sensitive volume

f = $R/2b$

L = Length of sensitive volume .

The effect of the curvature of the cylinder walls is small for particles whose range is small compared to b. Using a plane wall approximation, Robertson obtains

$$P(R) = \frac{R}{4}\left(\frac{2}{b} + \frac{2}{L}\right)$$

He shows this approximation to be very good for $f < 0.4$. Substituting the chamber parameters from Table 2, one obtains

$$P(R) = 0.086\ R$$

$$f = 0.318$$

Robertson has also shown that the correction due to the fact that the gamma source is close to one wall of the chamber and hence that the reactions are not uniformly distributed through the chamber is quite small.

Because they will only introduce second order errors the following assumptions are made:

(a) that the reaction is isotropic

(b) that the events are equally distributed in space

(c) that dE/dx is constant

(d) that the contribution of tracks entering the sensitive volume from the end regions is small.

For the case where the reaction produces particles of energy E_o (Range R_o), let the number of events taking place be N. Let No be the number of counts in the peak at energy E_o, and N(E)dE be the number of counts in an interval dE at energy E, range R.

From the definition of P(R) we have

$$N_o = N \left[1 - P(R_o) \right]$$

$$\therefore \quad N = \frac{N_o}{1 - P(R_o)} = \frac{N_o}{1 - 0.086R_o} \qquad \text{Eq. B-1}$$

From the assumption (c) we can write

$$\frac{dE}{dR} = \frac{E_o}{R_o}$$

$$\therefore \quad dR = \frac{R_o}{E_o} \, dE$$

$$\text{Now} \quad N(E)dE = N \left[P(R + dR) - P(R) \right]$$

$$= 0.086 \, NdR$$

$$= 0.086 \, N \frac{R_o}{E_o} \, dE$$

$$\therefore \quad N(E) = 0.086N \frac{R_o}{E_o} \text{ per Mev}$$

But since the calibration gives 14.3 channels per Mev

$$N(E) = 0.006N \frac{R_o}{E_o} \text{ per channel,} \qquad \text{Eq. B-2 .}$$

The range of a 5 Mev proton in argon at 100 p.s.i. absolute at 20°C happens to be 5.0 cms. Since the range of an alpha particle of the same energy is $1/8$ that of the proton, the constant R_o/E_o is taken as 1.0 for protons and 0.125 for alphas. The values of N and N(E) can now be obtained directly from Eqs. B-1 and B-2 as a function of N_o and E_o. The values have been computed and are given in Table 5.

APPENDIX C

CALCULATION OF THE CROSS SECTION

The expression used for calculating the cross section for the photodisintegration reaction is given by Robertson, 1963.

$$\sigma = \frac{\text{Yield}}{N \cdot H(d) \cdot \rho} \qquad \text{Eq. C-1}$$

where N = the effective gamma flux per steradian from the source

$H(d)$ = the effective solid angle-path length product for the chamber for a distance $(d + b)$ between the source and the centre axis of the chamber of radius b.

ρ = the atom density of argon in the chamber.

A. The Calculation of N

N can be obtained directly from the monitored gamma flux by application of Eq. C-2

$$N = \frac{N_c \, C_1 \, C_2 \, C_3}{\Omega} \qquad \text{Eq. C-2}$$

where N_c = total number of gamma rays counted by the gamma monitor during the experiment.

C_1 = corrective factor for the error in the lower level discriminator bias,

C_2 = corrective factor for the absorbtion of gammas in the target backing and in the chamber wall,

C_3 = corrective factor for the efficiency of the gamma counter,

Ω = the solid angle subtended at the target by the counter crystal face.

The error in the lower level discriminator bias was determined with the help of Figure 7. The actual discriminator cut off point was located with the calibrating pulser, and the half energy (8.8 Mev) point was obtained from the energy calibration (see Chapter III). Because the efficiency of the counter is given in terms of half energy bias, a correction factor of 1.068 was applied to Nc. This value for C_1 is the ratio of the number of counts recorded by the kicksorter between 8.8 and 19 Mev to the number actually passed by the low level discriminator.

The factor C_2 for the absorbtion of gamma rays in the target backing and the chamber wall was obtained with the help of absorption coefficients interpolated from the tables of Grodstein, 1957. The target backing was 0.1 mm of copper and the walls were 0.318 cm of mild steel (iron).

The gamma flux must therefore be reduced from the observed value in the ratio

$$C_2 = e^{-(\mu_c x_c + \mu_i x_i)} \qquad \text{Eq. C-3}$$

where μ_c = absorbtion coefficient for copper = 0.290 per cm

μ_i = absorbtion coefficient for iron = 0.245 per cm

x_c = thickness of copper = 0.01 cm

x_i = thickness of iron = 0.318 cm .

Substituting these figures in Eq. C-3 one obtains the value 0.90 for C_2.

The correction factor for the efficiency of the counter was discussed in Chapter III, where it was established that the value $C_3 = 100/81$ would be used.

The solid angle subtended by the target at the counter is readily calculated. The area of the crystal face is 38.5 cm^2 and its effective centre is 5.5 cm from the front of the counter (Singh, 1959). Since the latter was 82 cm from the target

$$\Omega = \frac{38.5}{(82+5.5)^2} = 5.04\ (10^{-3})\ \text{steradians}$$

The value of N is thus obtained from Eq. C-1

$$N = Nc\ (1.068)\ .\ (0.9)\ .\ \left(\frac{100}{81}\right)\ .\ \left(\frac{10^3}{5.04}\right) = 235\ Nc$$

but N_c = 3.15 (10^6) gammas (experimental figure)

$\therefore$ N = 7.4 (10^8) gammas per steradian.

B. Calculation of H(d)

Curves of $H(d)/V^{1/3}$ as a function of d with T as a parameter are given by Robertson, 1963, for an isotropic gamma source. The variables are

V = sensitive volume = 4.40 litres

b = chamber radius = 7.85 cms

L = length of sensitive volume = 22.7 cms

T = 2b/L = 0.692

d = distance from target to surface of sensitive volume = 3.5 cm.

Robertson's curve, obtained by numerical integration, gives H(d) = 31 cm-steradians for this case.

C. Calculation of ρ

At an absolute pressure of 103 p.s.i.a. and at 23°C

$$\rho = \frac{6.03\ (10^{23})}{22{,}400} \times \frac{103}{14.7} \times \frac{273}{296} \quad \text{atoms/cm}^3$$

$$\therefore \rho = 1.70\ (10^{20}) \quad \text{atoms/cm}^3 .$$

D. The Cross Section

The total cross section for the photoproduction of charged particles observed in this experiment can now be computed from Eq. C-1. The yield taken for this is the sum of the total number of counts associated with each peak as given in Table 5, plus 2000 contributed by peaks G, H, and J. The total cross section is therefore

$$\sigma = \frac{22,625}{(7.4(10^8)).(31).(1.7(10^{20}))} = 5.8 \text{ mb}$$

The partial cross section for the events associated with any given peak can be obtained by substituting the individual yield for the total one. If peaks A, B, G and H are attributed to photo alpha events the partial cross sections become

$$\sigma(\gamma,p) = 5.2 \text{ mb}$$

$$\sigma(\gamma,\alpha) = 0.6 \text{ mb} .$$

APPENDIX D

ENERGY LEVEL DIAGRAM

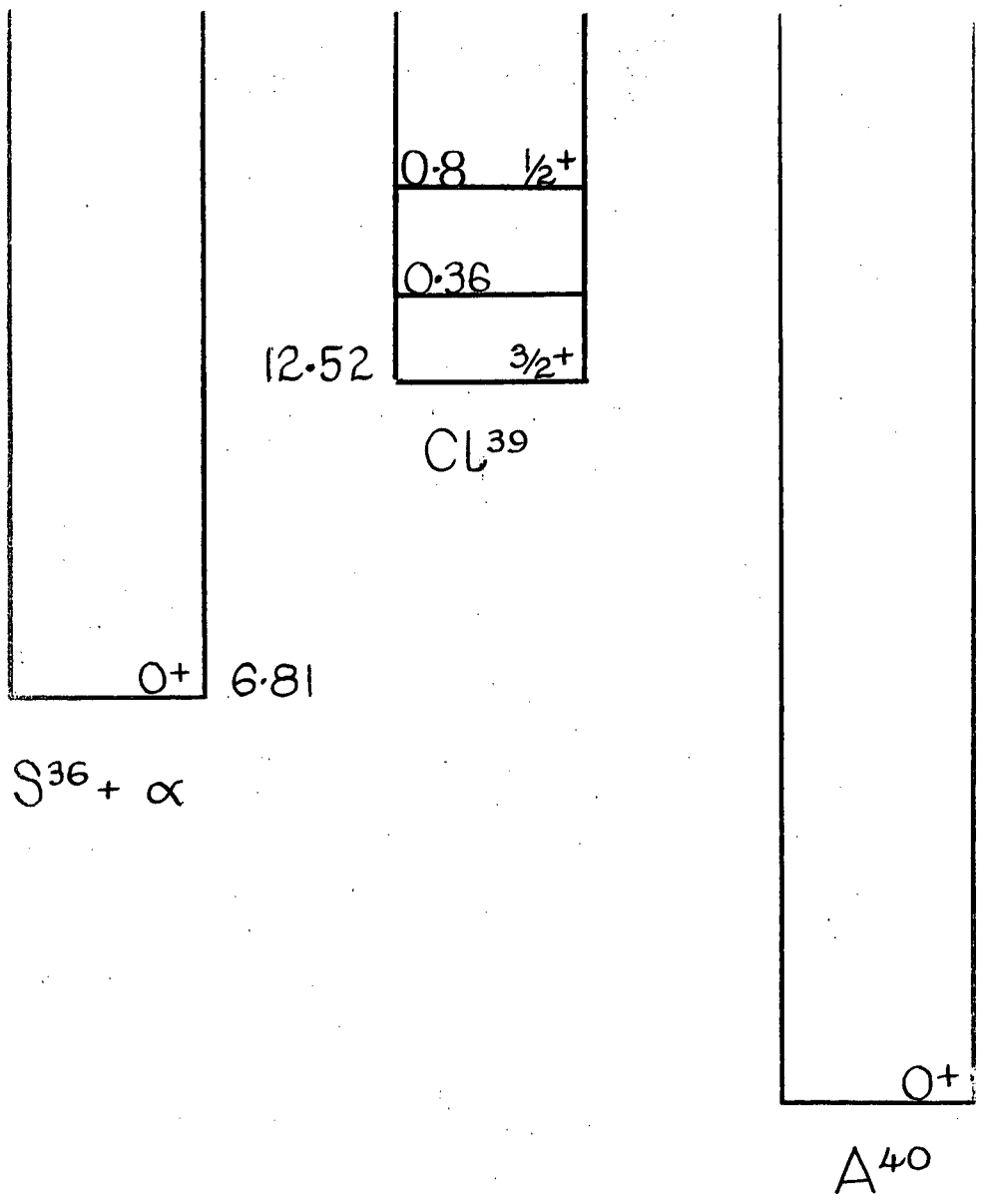

The energy levels shown here are those given by Endt and van der Leun, 1962. The mass differences are in Mev, and follow the tables of Everling et al, 1960.

BIBLIOGRAPHY

Bethe, H.A. (1937) Revs.Mod.Phys. 9, 69.

Blatt, J.M. and Weisskopf, V.F. (1952) Theoretical Nuclear Physics, (Wiley, New York).

Brix, P., Körding, A. and Lindenberger, K.H. (1959) Z.Physik 154, 569.

Bromley, D.A. and Rutlege, A.R. (1958) Nuclear Reaction Q-Values, (A.E.C.L. Chalk River, Ontario).

Colli, L. and Fachinni, U. (1952) Rev.Sci.Inst. 23, 39.

Courrant, E.D. (1950) Phys.Rev. 82, 703.

Dosch, H.G., Lindenberger, K.H. and Brix, P. (1960) Nuclear Physics 18, 615.

Diven, B.C. and Almy, G.M. (1950) Phys.Rev. 80, 407.

Drever, R.W.P. and Moljk, A. (1955) Phil.Mag. 46, 1337.

Emma, V., Milone, C., Rinzville, R. and Rubbino, A. (1959) Nuovo Cimento 14, 62.

Endt, P.M. and van der Leun, C. (1962) Nuclear Physics 34, 1.

Everling, F., König, L.A., Mattauch, J.H.E. and Wapstra, A.H. (1960) Nuclear Physics 18, 529.

Gillespie, A.B. (1953) Signal, Noise, and Resolution in Nuclear Counter Amplifiers, (McGraw-Hill, New York).

Goldhaber, M. and Teller, E. (1948) Phys.Rev. 74, 1046.

Grodstein, G.W. (1957) X-Ray Attenuation Coefficients from 10 keV to 100 Mev, N.B.S. Circular 583.

Gudden, F. and Eichler, J. (1958) Z.Physik 150, 436.

Hay, H.J. and Warren, J.B. (1959) Can.J.Phys. 37, 1153.

Heywood, D.R. (1960) M.A. Sc. Thesis, U.B.C.

Hirzel, O. and Wäffler, H. (1947) Helv.Phys.Acta 20, 373.

Iavor, I.P. (1958) Soviet Physics J.E.T.P. 34, 983.

Jensen, P. (1948) Naturwiss. 35, 190.

Komar, A.P., Bochagov, B.A. and Solyakin, G.E. (1961)
Dokl. Akad. Nauk. 141, 1339.

McPherson, D., Pederson, E. and Katz, L. (1954)
Can.J.Phys. 32, 593.

Mainsbridge, B. (1960) Austr.J.Phys. 13, 204.

Mainsbridge, B. (1960) Nuclear Physics 21, 1.

Monier, L.F. (1960) M.A. Sc. Thesis, U.B.C.

Morrow, R.A. (1958) M.Sc. Thesis, U.B.C.

Robertson, L.P. (1957) M.A. Thesis, U.B.C.

Robertson, L.P. (1963) Ph.D. Thesis, U.B.C.

Schiff, L.I. (1948) Phys.Rev. 73, 1131.

Scott, J.M.C. (1954) Phil.Mag. 45, 441.

Sharpe, J. (1955) Nuclear Radiation Detectors
(Methuen Monograph)

Singh, P.P. (1959) Ph.D. Thesis, U.B.C.

Spicer, B.M. (1955) Phys.Rev. 100, 791.

Toms, M.E. and Stephens W.E. (1953) Phys.Rev. 92, 362.

Toms, M.E. (1955) Bibliography of Photonuclear Reaction
Naval Research Laboratory, Washington, D.C.

Weisskopf, V.F. (1937) Phys.Rev. 52, 295.

Weisskopf, V.F. and Ewing, D.H. (1940) Phys.Rev. 57, 472.

Wilkinson, D.H. and Carver, J.H. (1951) Phys.Rev. 83, 466.